Ab Initio/RRKM Study of the $O(^1D) + NH_3$ Reaction: Prediction of Product Branching Ratios

Ling Wang,[†] Alexander M. Mebel,*[,‡,§] Xueming Yang,[†] and Xiuyan Wang*[,†]

State Key Laboratory of Molecular Reaction Dynamics, Dalian Institute of Chemical Physics, Chinese Academy of Science, Dalian 116023, People's Republic of China, Department of Chemistry and Biochemistry, Florida International University, Miami, Florida 33199, and Institute of Atomic and Molecular Sciences, Academia Sinica, P.O. Box 23-166, Taipei 10764, Taiwan

Received: September 14, 2004; In Final Form: October 20, 2004

The reaction mechanism, rate constants, and product branching ratios for the $O(^1D) + NH_3$ reaction have been studied using ab initio/RRKM methods. The reaction is shown to occur mainly through the insertion mechanism involving the long-lived chemically activated NH_2OH^* intermediate. The calculated branching ratios of various decomposition products of NH_2OH^* are in good agreement with recently reported experimental values. The reaction can also proceed through the addition/abstraction mechanism on the first excited-state PES, which is demonstrated to provide some contribution to the $NH_2 + OH$ channel and to partially account for the forward scattering of the OH products observed in experiment.

1. Introduction

The chemistry of ammonia with an oxygen atom (^3P or ^1D) is very complex and involves many intermediate fast reactions, and, in some cases, neither the products nor the rate constants are well-known. These reactions play an important role in the conversion of fuel-nitrogen to the atmospheric contaminant NO.[1] The $O(^3P) + NH_3$ reaction has been extensively studied using a wide variety of detection techniques and a broad range of temperatures in experiments. A theoretical investigation of this reaction was also carried out most recently by Espinosa-Garcia,[2] who considered the H-atom abstraction mechanism. In addition to the $O(^3P) + NH_3$ reaction, the vibrationally mediated photodissociation of NH_2OH was studied both experimentally and theoretically.[3]

The crossed molecular beam investigation of the $O(^1D) + NH_3$ reaction has been performed by Shu et al.[4] Two different reaction channels, $OH + NH_2$ and $NHOH/NH_2O + H$, have been observed. The formation of OH was found to be the dominant process, while the H formation process is minor. There are also other possible minor channels for this reaction, such as the H_2O and H_2 formation channels. From the experimental data, it is not clear how significant these reaction channels are relative to the OH formation channel, so the determination of the branching ratios of all possible reaction pathways remains an important task. However, no theoretical study of the rate constants and product branching ratios for the $O(^1D) + NH_3$ reaction has been reported so far, to our knowledge, although the heats of formation for various reaction products, including the H_2NO and HNOH radicals, were calculated by Nguyen et al.[5] and Lin et al.[6]

In this paper, we apply the ab initio/RRKM approach to study the $O(^1D) + NH_3$ reaction. We use high level ab initio methods to compute the reaction potential energy surface (PES). The ab initio results are then employed to calculate microcanonical RRKM rate constants for various channels. One of the important results of this study is the finding that the abstraction mechanism for the OH formation channel in the $O(^1D) + NH_3$ reaction can take place through a short-lived complex, H_2NH-O (C_s,$^1A''$), on the first excited singlet PES, contributing to the OH radical forward scattering observed in the experiment.[4]

2. Computational Details

For the ground electronic state, the geometry of equilibrium structures and transition states of various species has been optimized by employing the hybrid density functional B3LYP method[7,8] with the 6-311G(d,p) basis set. Vibrational frequencies calculated at the B3LYP/6-311G(d,p) level were used for characterization of the stationary points and zero-point energy (ZPE) corrections. To obtain more accurate energies on the PES, we employed the CCSD(T)[9] method with the large 6-311+G(3df,2p) basis set. The CCSD(T)/6-311+G(3df,2p)//B3LYP/6-311G(d,p) + ZPE[B3LYP/6-311G(d,p)] calculational scheme[10] has been shown to provide accuracies of 1−2 kcal/mol for atomization energies of the G2 test set of molecules. Such accuracy is also expected for other molecules, unless their wave functions exhibit a strong multireference character. A similar CCSD(T)//B3LYP approach has also been demonstrated to be accurate for transition state energies.[11]

For the first excited singlet electronic state of the H_2NH-O species, geometry optimization and calculations of vibrational frequencies of stationary points have been carried out using the complete active space self-consistent field (CASSCF) method[12,13] with the 6-311G(d,p) basis set. We used the full-valence active space including 14 electrons distributed on 11 orbitals ($8A' + 3A''$ within C_s symmetry). The energies of optimized excited-state structures were then refined by employing internally contracted multireference configuration interaction (MRCI)[14,15] calculations with the same active space in conjunction with the 6-311+G(3df,2p) and Dunning's augmented correlation consistent valence triple-ζ (aug-cc-pVTZ) basis sets.[16] The latter

* Corresponding author. (A.M.M.) Fax: +1-305-348-3772. E-mail: mebela@fiu.edu. (X.W.) Fax: +86-411-467-5584. E-mail: wangxy@dicp.ac.cn.
† Chinese Academy of Sciences.
‡ Florida International University.
§ Academia Sinica.

10.1021/jp0458452 CCC: $27.50
Published on Web 12/04/2004

TABLE 1: Total Energies (hartrees) and Relative Energies (kcal/mol) for Various Species Calculated at the CCSD(T)/6-311+G(3df,2p), MRCI/6-311+G(3df,2p), and MRCI/aug-cc-pVTZ Levels of Theory

	total energy			relative energy		
species	CCSD(T)	CCSD(T)+ZPE	ZPE[a]	CCSD(T)	CCSD(T)+ZPE	CCSD(T)+ZPE[b]
$O(^1D) + NH_3$	−131.36139	−131.32707	0.03432	0.0	0.0	0.0
$NH_2OH(^1A')$	−131.53617	−131.49587	0.04030	−109.7	−105.9	−100.1
$NH_2 + OH$	−131.42859	−131.40128	0.02732	−42.2	−46.6	−40.7
$H_2NO + H$	−131.40474	−131.37832	0.02642	−27.2	−32.2	−26.3
cis-HNOH + H	−131.38466	−131.35858	0.02607	−14.6	−19.8	−13.9
trans-HNOH + H	−131.39364	−131.36659	0.02705	−20.3	−24.8	−19.0
TS5	−131.42300	−131.38769	0.03531	−38.7	−38.0	−32.2
TS6	−131.38399	−131.35546	0.02853	−14.2	−17.8	−12.0
$NOH(^3A'') + H_2$	−131.42961	−131.40585	0.02377	−42.8	−49.4	−43.6
$NOH(^1A') + H_2$	−131.40127	−131.37795	0.02332	−25.0	−31.9	−26.1
$NH\ (^1\Delta) + H_2O$	−131.40042	−131.37163	0.02879	−24.5	−28.0	−22.1
$HN\cdots OH_2$	−131.43574	−131.39921	0.03653	−46.7	−45.3	−39.4
	MRCI+Q[c]	MRCI+ZPE		MRCI+Q[c]	MRCI+ZPE	
$O(^1D)\cdots NH_3$[d,e]	−131.41116	−131.37686	0.03430	0.0	0.0	
$O(^1D)\cdots NH_3$[d,f]	−131.41074	−131.37644	0.03430	0.0	0.0	
$H_2NH-O(^1A'')$[e]	−131.41199	−131.37749	0.03450	−0.5	−0.4	
$H_2NH-O(^1A'')$[f]	−131.41028	−131.37578	0.03450	0.3	0.4	
$TS7(^1A'')$[e]	−131.40502	−131.37322	0.03180	3.9	2.3	
$TS7(^1A'')$[f]	−131.40286	−131.37106	0.03180	4.9	3.4	
$NH_2OH(^1A')$[e]	−131.57884	−131.53854	0.04030	−105.2	−101.5	
$NH_2OH(^1A')$[f]	−131.57714	−131.53684	0.04030	−104.4	−100.7	

[a] ZPE (hartrees) are calculated at the B3LYP/6-311G(d,p) level for the species on the ground-state PES and at the CASSCF/6-311G(d,p) level for the H_2NH-O complex and TS7 on the excited $^1A''$ PES. [b] Corrected relative energies computed using the total energy of $O(^1D) + NH_3$ calculated from the total energy of $O(^3P) + NH_3$ at the CCSD(T)/6-311+G(3df,2p) level and experimental energy difference between $O(^1D)$ and $O(^3P)$. [c] Including Davidson's correction for quadruple excitations. Core electrons were also included in the MRCI calculations. [d] The energy of $O(^1D) + NH_3$ is calculated for the supermolecule consisting of the oxygen atom and ammonia separated by 100 Å. [e] Calculated with the aug-cc-pVTZ basis set. [f] Calculated with the 6-311+G(3df,2p) basis set.

was used for the excited-state calculations because it includes more diffuse functions and therefore is expected to describe the excited $^1A''$ wave function slightly more accurately. The MOLPRO 2002,[17] DALTON 1.2,[18] and GAUSSIAN 98[19] programs were used for calculations.

Rate constants for individual unimolecular reaction steps were computed using RRKM theory.[20−22] The total available internal energy in RRKM calculations was taken as the energy of chemical activation (e.g., the energy released in the $O(^1D) + NH_3 \rightarrow NH_2OH$ reaction) plus the experimental collision energy of 7.1 kcal/mol.[4] In particular, the available internal energy of the NH_2OH intermediate was taken as 107.2 kcal/mol. For some decomposition channels, which do not have exit barriers on the PES, for instance, decomposition of NH_2OH leading to $NH_2 + OH$, $H_2NO + H$, or *cis*/*trans*-HNOH + H, the microcanonical variational transition state theory (MVTST)[22] was employed. The transition state position was determined by minimization of rate constants along the reaction coordinate, which was chosen as the length of the breaking N−O, O−H, and N−H bonds, respectively. The B3LYP/6-311G(d,p) method was used to scan the PES along the reaction coordinate (R_C) and to compute $3N - 7$ vibrational frequencies projected out of the gradient direction. The energies of the variational transition states were then refined using the CCSD(T)/6-311+G(3df,2p) method. The detailed protocol for RRKM and MVTST calculations has been described in our earlier works.[23−25]

3. Results and Discussion

Table 1 presents total and relative energies for various species, while their unscaled vibrational frequencies are collected in Table 2. Table 3 contains energies and molecular parameters for variational transition states obtained using the MVTST approach. Rate constants for various channels calculated using RRKM theory are presented in Table 4. Optimized geometries for intermediates and transition states are shown in Figure 1. Figure 2 contains optimized geometries for stationary points on the first excited-state PES. Profiles of the ground and first excited $^1A''$ PES are depicted in Figure 3. Figure 4 shows the potential energy curves E(VTS) and variational rate constants k(VTS) versus R_C for the four variational transition states.

3.1. $O(^1D) + NH_3$ Reaction Involving Vibrationally Excited NH_2OH^* Intermediate. *3.1.1. Potential Energy Surface.* According to our calculations, the $O(^1D) + NH_3$ reaction in the ground electronic state produces a long-lived vibrationally excited intermediate NH_2OH^* without an entrance barrier. This result is in accord with a very high rate constant for the reaction, 2.51×10^{-10} cm^3 molecule^{-1} s^{-1} measured at 200−300 K, and the fact that the rate constant exhibits no detectable temperature dependence.[26,27] To reproduce the experimental value theoretically, one needs to carry out variational RRKM calculations for the critical minimal energy reaction path $O(^1D) + NH_3 \rightarrow NH_2OH$. However, because our main target here is to predict product branching ratios for the NH_2OH decomposition, which are independent of the rate of its formation from the $O(^1D) + NH_3$ reactants, we do not pursue such RRKM calculations in this study. The C_s-symmetric NH_2OH molecule resides in a deep well, 105.9 kcal/mol below the reactants at the CCSD(T)/6-311+G(3df,2p)//B3LYP/6-311G(d,p) level (102.8 kcal/mol according to experimental heats of formation of the reactants[28] and NH_2OH[29]). The deviation is caused by the multireference character of the wave function for $O(^1D)$, which is not properly described at the CCSD(T) level. Indeed, the $O(^1D)-O(^3P)$ energy gap is calculated as 51.2 kcal/mol at CCSD(T)/6-311+G(3df,2p), which significantly overestimates the experimental value of 45.3 kcal/mol.[28] Wave functions of $O(^3P) + NH_3$ and NH_2OH both have a single-reference character, and their energies are properly described by the CCSD(T) method. Therefore, more accurate relative energies can be predicted if

TABLE 2: Vibrational Frequencies (in cm^{-1}) for Various Species and Transition States Calculated at the B3LYP/6-311G(d,p) Level of Theory

species	frequencies (in cm^{-1})
$NH_3(C_{3v},{}^1A_1)$	1071.3(a_1), 1682.0(e), 1682.0(e), 3460.1(a_1), 3579.2(e), 3579.2(e)
$NH_2(C_{2v},{}^2B_1)$	1535.2(a_1), 3332.3(a_1), 3417.7(b_2)
$OH(C_{\infty v},{}^2\Pi)$	3704.7(σ)
$NH(C_{\infty v},{}^1\Delta)$	3279.7(σ)
$H_2O(C_{2v},{}^1A_1)$	1638.5(a_1), 3810.3(a_1), 3907.4(b_2)
$H_2(D_{\infty h},{}^1\Sigma_g)$	4419.3(σ_g)
$NOH(C_s,{}^3A'')$	1119.2(a′), 1233.5(a′), 3659.9(a′)
$NOH(C_s,{}^1A')$	1272.9(a′), 1482.0(a′), 3059.8(a′)
$NH_2OH(C_s,{}^1A')$	417.6(a″), 933.0(a′), 1151.5(a′), 1328.6(a″), 1406.8(a′), 1673.1(a′), 3436.9(a′), 3512.1(a″), 3828.1(a′)
$HN\cdots OH_2(C_s,{}^1A')$	345.0(a″), 466.1(a′), 625.7(a″), 689.4(a′), 1266.7(a′), 1617.1(a′), 3356.8(a′), 3798.1(a′), 3885.2(a″)
$TS5(C_s,{}^1A')$	650.5i(a′), 436.1(a″), 489.9(a′), 705.3(a″), 1319.1(a′), 1553.4(a′), 3298.2(a′), 3781.9(a′), 3914.7(a″)
$TS6(C_1,{}^1A)$	866.2i, 448.7, 671.5, 942.2, 1043.4, 1176.9, 1415.7, 3312.2, 3512.2
$H_2NO(C_s,{}^2A')$	315.4(a′), 1279.1(a″), 1378.1(a′), 1679.6(a′), 3409.0(a′), 3532.8(a″)
cis-$HNOH(C_s,{}^2A'')$	544.2(a″), 1101.7(a′), 1297.3(a′), 1509.3(a′), 3280.8(a′), 3710.9(a′)
trans-$HNOH(C_s,{}^2A'')$	758.0(a″), 1114.7(a′), 1266.5(a′), 1579.7(a′), 3363.5(a′), 3785.4(a′)
$H_2NH-O(C_s,{}^1A'')$[a]	53.8(a′), 68.6(a″), 86.9(a′), 1192.9(a′), 1714.3(a′), 1715.8(a″), 3356.2(a′), 3474.1(a″), 3480.6(a′)
$TS7(C_s,{}^1A'')$[a]	2451.8i(a′), 433.1(a′), 472.2(a″), 1294.8(a′), 1400.0(a′), 1527.9(a′), 1637.4(a″), 3498.3(a′), 3694.2(a″)

[a] Frequencies at the CASSCF/6-311G(d,p) level obtained using the DALTON program.

TABLE 3: Breaking Bond Distances, Relative Energies (in kcal/mol), and Frequencies (in cm^{-1}) for Variational Transition States Calculated Using the Microcanonical Variational Transition State Theory

species	R_C, Å	relative energy[a]	rotational constants, GHz	frequencies, cm^{-1}
$NH_2O-H(C_s,{}^1A')$	1.8	−29.1	128.1, 26.9, 25.6	548.5(a″), 628.0(a′), 723.4(a′), 1285.3(a′), 1295.0(a″), 1678.9(a′), 3411.5(a′), 3532.5(a″)
H−NHOH(cis)	2.2	−17.3	95.4, 25.0, 22.8	415.2, 463.7, 638.5, 1079.8, 1306.2, 1507.7, 3312.3, 3706.4
H−NHOH(trans)	2.2	−22.2	95.6, 25.1, 22.9	444.8, 458.9, 798.2, 1091.9, 1274.1, 1580.0, 3386.2, 3779.6
$H_2N-OH(C_s,{}^1A'')$	2.2	−53.7	203.5, 12.5, 12.4	372.6(a″), 407.6(a′), 564.7(a″), 624.9(a′), 1545.6(a′), 3315.1(a′), 3396.8(a′), 3478.9(a″)

[a] Calculated at the CCSD(T)/6-311+G(3df,2p)//B3LYP/6-311G(d,p) level, with respect to the $O(^1D) + NH_3$ limit.

TABLE 4: Calculated Microcanonical Rate Constants (in s^{-1}) and Branching Ratio (%)

reaction	rate constant	branching ratio
(k_{v1}) $NH_2OH \rightarrow H_2NO + H$	1.74×10^{11}	2.34
(k_{v2}) $NH_2OH \rightarrow$ *cis*-$HNOH + H$	4.77×10^{10}	0.64
(k_{v3}) $NH_2OH \rightarrow$ *trans*-$HNOH + H$	9.44×10^{10}	1.27
(k_{v4}) $NH_2OH \rightarrow NH_2 + OH$	6.66×10^{12}	89.54
(k_5) $NH_2OH \rightarrow HN\cdots H_2O$	4.54×10^{11}	6.10
(k_6) $NH_2OH \rightarrow NOH + H_2$	7.70×10^{9}	0.10
(k_{exc}) $H_2NH-O \rightarrow NH_2 + OH$	9.94×10^{10}	
(k_{-5}) $HN\cdots H_2O \rightarrow NH_2OH$	4.54×10^{12}	

we take the relative energy of NH_2OH with respect to $O(^3P) + NH_3$ and correct this value using the experimental energy difference between $O(^3P)$ and $O(^1D)$. The well depth at NH_2-OH is then evaluated as 100.1 kcal/mol, 2.7 kcal/mol lower than the experimental data, but we have to keep in mind that the uncertainty of the recommended heat of formation for NH_2-OH (−7.2 kcal/mol) is ±2.2 kcal/mol. In this view, the accuracy of our method can be considered as satisfactory. The accuracy of this approach is also confirmed by the MRCI/6-311+G(3df,-2p) and MRCI/aug-cc-pVTZ calculations for the NH_2OH intermediate. At these levels, the relative energy of this molecule with respect to the $O(^1D) + NH_3$ reactants is computed as −100.7 and −101.5 kcal/mol, respectively, in close agreement with the empirically corrected CCSD(T)/6-311+G(3df,2p) result (−100.1 kcal/mol) and the experimental value (−102.8 kcal/mol).

Six pathways lead from NH_2OH to various decomposition products. The channels producing $NH_2 + OH$, *cis*/*trans*-HNOH + H, and $H_2NO + H$ products by the N−O, N−H, and O−H bond cleavage do not have exit barriers, because the reverse reactions are barrierless recombinations of two radicals with the formation of a single bond. Using the corrected energy for $O(^1D)$ (the CCSD(T)/6-311+G(3df,2p) calculated energy of $O(^3P)$ + experimental $O(^1D)-O(^3P)$ energy difference, see Table 1), we obtain the exothermicities of the $NH_2 + OH$, *cis*-HNOH + H, *trans*-HNOH + H, and $H_2NO + H$ products as 40.7, 13.9, 19.0, and 26.3 kcal/mol, respectively. For $O(^1D) + NH_3 \rightarrow NH_2 + OH$, our result is close to the experimental value of 40.6 kcal/mol. No experimental heats of formation are available to our knowledge for the isomers of the H_2NO species. The best theoretical estimates are given by Nguyen and co-workers[5] as 18.3 and 24.8 kcal/mol for H_2NO and *trans*-HNOH, respectively. Using these values together with experimental $\Delta H_f(0\ K)$, the heats of the $O(^1D) + NH_3 \rightarrow H_2NO + H$ and $O(^1D) + NH_3 \rightarrow$ *trans*-HNOH + H reactions are obtained as −25.2 and −18.7 kcal/mol, respectively, which are similar to our results.

To calculate rate constants for the barrierless bond cleavage reaction channels, we used the MVTST approach[22−25] and

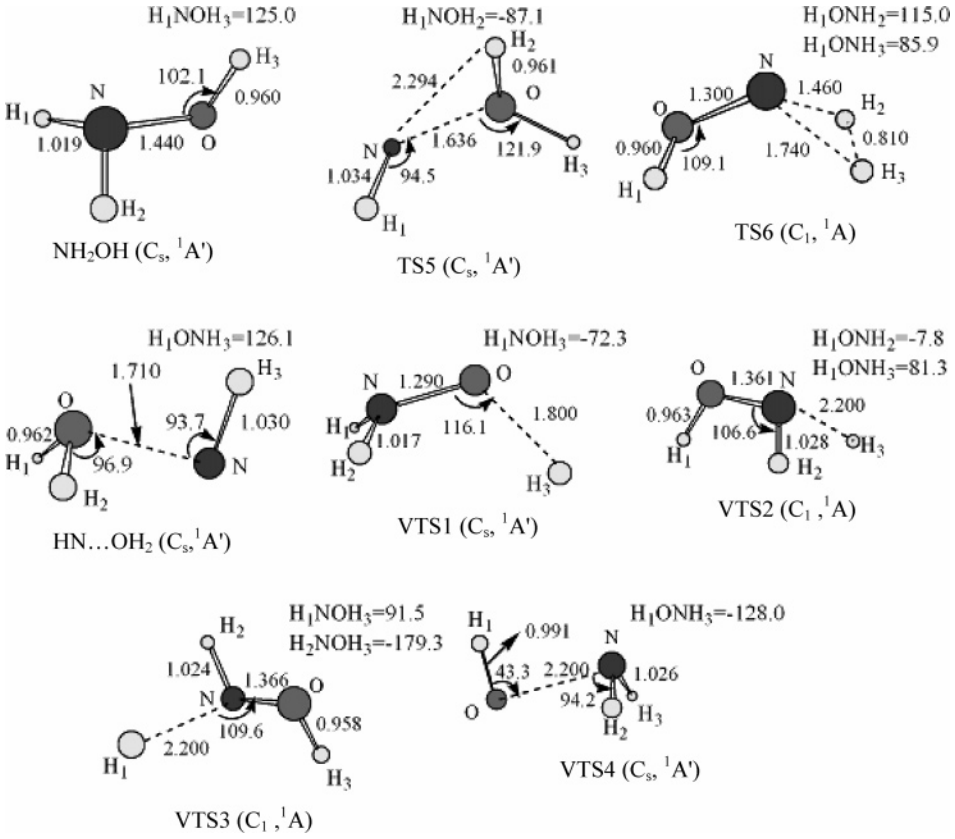

Figure 1. Optimized geometries of intermediates and transition states on the ground-state potential energies surface calculated at the B3LYP/6-311G(d,p) level of theory (bond lengths are in angstroms, bond angles are in degrees).

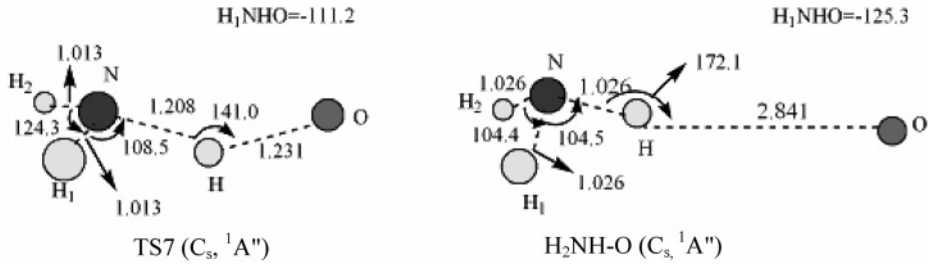

Figure 2. Optimized geometries for stationary points on the first excited singlet state PES calculated at the CASSCF/6-311G(d,p) level of theory (bond lengths are in angstroms, bond angles are in degrees).

scanned PES along the breaking bond while optimizing all other geometric parameters. In such a way, we located four variational transition states VTS1−VTS4 corresponding to the NH_2O + H, *cis*-NHOH + H, *trans*-NHOH + H, and H_2N + OH channels (see Figure 1 and Table 3). The E(VTS) and k(VTS) curves versus R_C for the four variational transition states are plotted in Figure 4. The variational barrier heights are found to be 71.0, 82.8, 77.9, and 46.3 kcal/mol, respectively. These values are somewhat lower than the calculated strengths of the corresponding O−H, N−H (cis), N−H (trans), and N−O bonds, 73.8, 86.2, 81.1, and 59.4 kcal/mol, respectively. The difference between the bond strength and the variational barrier is largest for the N−O bond cleavage, indicating that VTS4 is the tightest transition state among the four loose variational transition states. It should be noted that two N−H bonds in NH_2OH are actually equivalent and the difference in variational barriers originates from the energy difference in energies for the cis and trans isomers of HNOH.

Distinct transition states exist for the other two reaction channels leading to $NOH(^1A') + H_2$ and $NH(^1\Delta) + H_2O$. The former occurs via TS6 by a 1,1-H_2 elimination with a barrier of 88.1 and 14.1 kcal/mol in the forward and reverse directions,

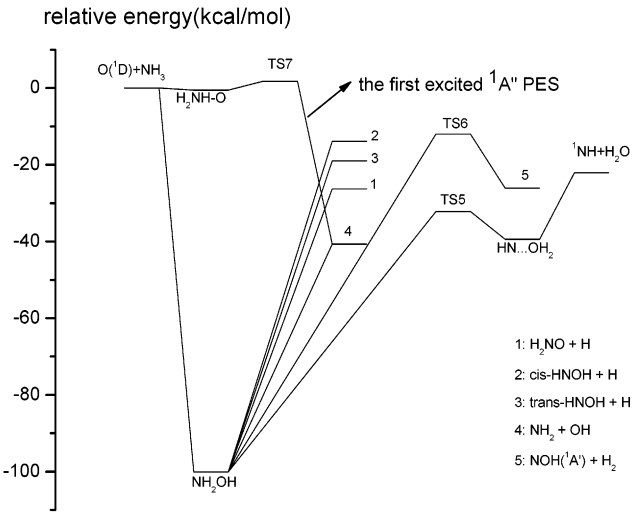

Figure 3. Potential energy diagram for the $O(^1D) + NH_3$ reaction. The ground-state PES is constructed using the CCSD(T)/6-311+G-(3df,2p) method, and the first excited-state PES is constructed using the MRCI/aug-cc-pVTZ method.

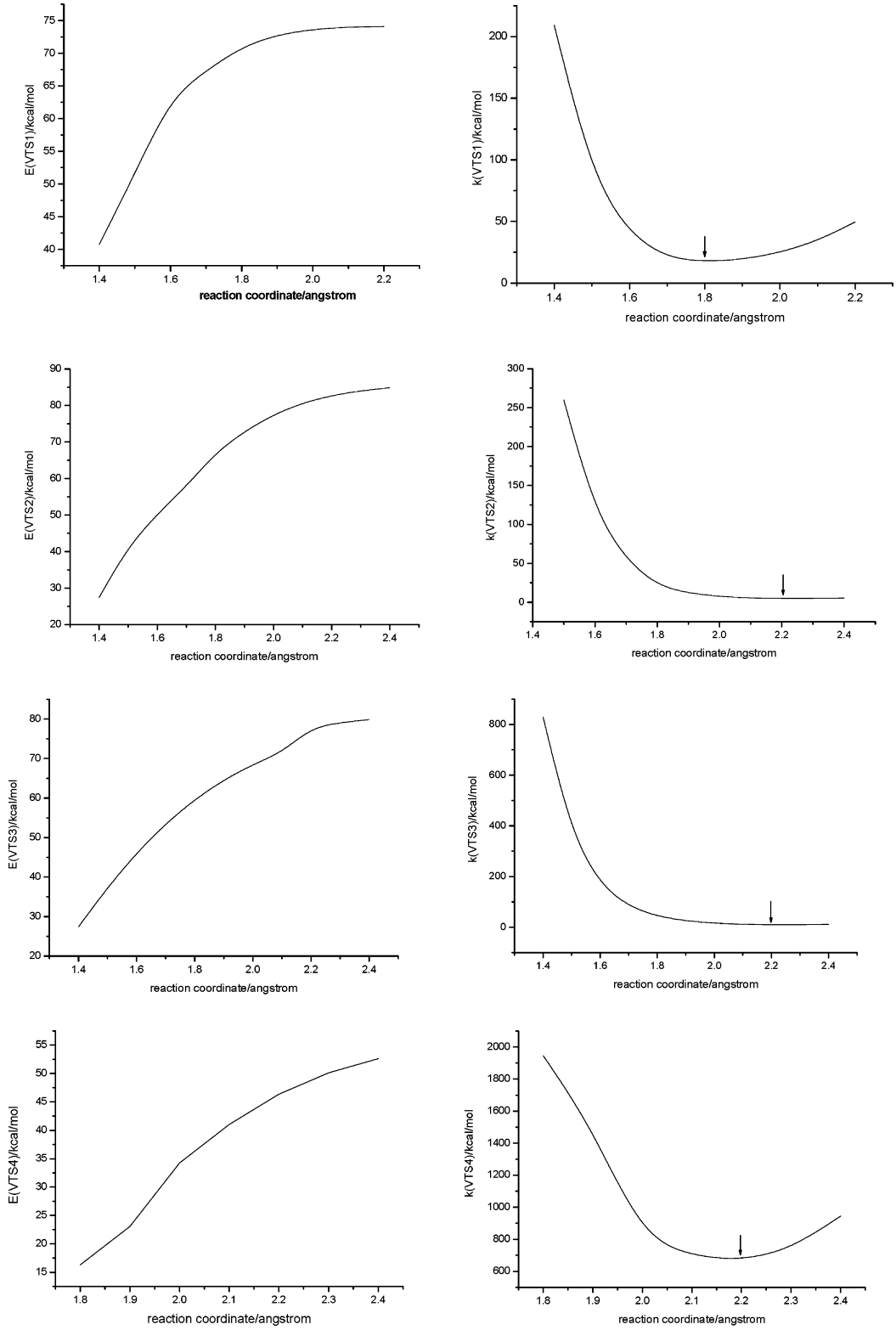

Figure 4. E(VTS) versus R_C and k(VTS) versus R_C curves used for the variational transition state searches. Arrows show the positions of variational transition states.

respectively; the NOH(^{1}A′) + H_2 product channel is 26.1 kcal/mol exothermic with respect to O(^{1}D) + NH_3. ^{1}A′ is the first excited electronic state for NOH, and the equilibrium structure in the ground ^{3}A″ state lies 17.5 kcal/mol lower in energy than NOH(^{1}A′). However, the NH_2OH(^{1}A′) → NOH(^{3}A″) + H_2 dissociation is spin-forbidden, and the process occurring via TS6 leads to the electronically excited NOH(^{1}A′) product. The HNO-(^{1}A′) molecule, which corresponds to the global minimum for the triatomic [H,N,O] systems, is 24.7 and 42.2 kcal/mol more stable than NOH(^{3}A″) and NOH(^{1}A′), respectively. In principle, HNO could be produced by 1,2-H_2 elimination from NH_2OH. However, a careful search of a transition state for this process was not successful; the calculations converged to TS6, and we conclude that NH_2OH is not likely to decompose directly to HNO + H_2.

The NH_2OH → HN···OH_2 → NH($^1\Delta$) + H_2O channel initially proceeds via TS5 by H migration from NH_2 to OH in conjunction with N−O bond lengthening leading to a HN···

OH_2 complex. For this step, the barriers are calculated as 67.9 and 7.2 kcal/mol in the forward and reverse directions, respectively. The $HN\cdots OH_2$ complex is bound by 17.3 kcal/mol through a dative N−O bond and can dissociate barrierlessly without a well-defined TS to the $NH(^1\Delta) + H_2O$ products. The $NH(^1\Delta) + H_2O$ product channel is 22.1 kcal/mol exothermic (24.3 kcal/mol according to experiment[28]). Although the NH molecule in the ground $^3\Sigma^-$ state is 36.3 kcal/mol more favorable than $NH(^1\Delta)$,[28] the $NH(^3\Sigma^-) + H_2O$ channel is spin-forbidden and can take place only through singlet−triplet intersystem crossing.

On the basis of the computed activation barrier, we can expect $NH_2 + OH$ to be the major reaction products. Our RRKM calculations described below allow us to support this qualitative conclusion with calculated relative branching ratios.

3.1.2. Microcanonical Rate Constants and Product Branching Ratios. The scheme chosen for the kinetics calculations is as follows:

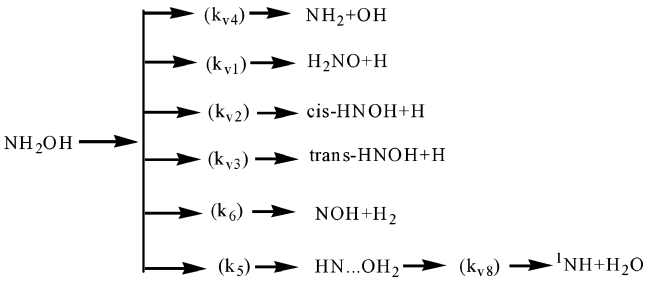

and the calculated microcanonical rate constants are presented in Table 4. To compare our calculated branching ratios with those obtained in experiment, the experimental collision energy of 7.1 kcal/mol[4] was included into available internal energy. The $NH_2OH \rightarrow NH_2 + OH$ channel is found to have the largest rate constant k_{v4} of 6.66×10^{12} s^{-1}, and $NH_2OH \rightarrow NOH + H_2$ has the smallest rate constant k_6 of 7.70×10^9 s^{-1}. The k_{v4} value approaches the applicability limit of the RRKM theory, 10^{13} s^{-1}, which assumes that the species are vibrationally equilibrated, as the time scale of the vibrational relaxation, in general, is in the picosecond or subpicosecond range. If some rate constant exceeds 10^{13} s^{-1}, this indicates that the basic assumption of the RRKM theory of a statistical distribution of the vibrational energy over all modes can break down, and such high unimolecular rates can lead to non-RRKM (nonstatistical) behavior of the system.[20]

We tried to calculate variational rate constant k_{v8} for the decomposition of $HN\cdots OH_2$ considering the N···O distance as the reaction coordinate; however, the computed rates exceed 10^{13} s^{-1} and do not reach a minimal value even at N···O values larger than 4 Å. This indicates that k_{v8} is very high and, once the $HN\cdots OH_2$ complex is formed via TS5, it can readily decompose to $NH + H_2O$; that is, the $NH_2OH \rightarrow HN\cdots OH_2$ step is rate-limiting for the H_2O formation channel. Using the steady-state approximation for the $HN\cdots OH_2$ intermediate, we obtain the rate constant for the H_2O formation channel as $k_{5'} = k_5k_{v8}/(k_{-5} + k_{v8})$, and, assuming that k_{v8} is very high, $k_{v8} \gg k_{-5}$, we can conclude that $k_{5'} \approx k_5$. A similar conclusion was made recently for the $CH_3OH \rightarrow H_2C\cdots OH_2 \rightarrow CH_2 + H_2O$ channel of the methanol decomposition where the isomerization of CH_3OH to the $H_2C\cdots OH_2$ complex was also shown to be the rate-determining step for the H_2O formation.[30]

Using the calculated rate constants, we computed the relative branching ratios to be 89.54% for the $NH_2OH \rightarrow NH_2 + OH$ channel, 4.25% for the H formation channel, 6.10% for the NH_2-$OH \rightarrow NH + H_2O$ channel, and 0.1% for the $NH_2OH \rightarrow NOH + H_2$ channel. Thus, the OH formation channel is the most important in the $O(^1D) + NH_3$ reaction involving the NH_2OH^* complex. The calculated branching ratios are in good agreement with 90% for the OH formation and 10% for H formation obtained in experiment. This result implies that these products are expected to be formed through the vibrationally excited NH_2-OH^* intermediate, which is produced by the insertion mechanism. The $NH + H_2O$ and $NOH + H_2$ channels have small contributions according to our calculations, but were not found in experiment.[4] The fact that the H_2O formation channel was not observed can be due to the difficulties in distinguishing the signals from H_2O in mass spectra in the presence of the NH_3 reactant as the two molecules have similar masses, while the H_2 formation channel is indeed very minor. In experiment,[4] it is also found that OH radical is partly forward scattered relative to the $O(^1D)$ beam direction. The forward-scattered OH products can be either formed by the insertion mechanism on the ground-state PES via a short-lived NH_2OH complex, which is a dynamics effect, or produced by an alternative abstraction mechanism on the first excited PES, as we recently demonstrated for the $O(^1D) + SiH_4$ reaction.[31] Therefore, we additionally investigated the lowest excited singlet electronic state for the NH_3O system.

3.2. Addition/Abstraction Mechanism for the $O(^1D) + NH_3$ Reaction. A profile of the first excited singlet state PES for the addition/abstraction mechanism calculated using the MRCI/aug-cc-pVTZ//CASSCF/6-311G(d,p) approach is drawn in Figure 3. At this theoretical level, a local minimum, the H_2-NH−O complex (C_s,$^1A''$), lies 0.4 kcal/mol lower in energy than $O(^1D) + NH_3$. TS7 connecting the complex with the $NH_2 + OH$ products also has C_s symmetry and $^1A''$ electronic state. The calculated energy difference between the reactants and the complex is rather low, so the existence of H_2NH-O ($^1A''$) as a local minimum on the first excited PES could be an artifact of the theoretical method used. This may be a case because the CASSCF method employed for the geometry optimization does not account for dynamical correlation energy. As seen in Table 1, the MRCI/6-311+G(3df,2p)//CASSCF/6-311G(d,p) calculations give a slightly positive relative energy (+0.4 kcal/mol) of H_2NH-O ($^1A''$) with respect to the reactants, also indicating that this complex may not exist. If the complex does exist on the excited $^1A''$ PES, the addition/abstraction mechanism involves initial addition of the $O(^1D)$ atom to the NH_3 molecule along one of the N−H bonds. The O atom then continues to approach H, the N−H bond distance increases, and the O−H bond begins to form. After passing TS7, the N−H bond is completely broken, and the O−H bond is formed to lead to the $NH_2 + OH$ products. At the MRCI/aug-cc-pVTZ level of theory, the H_2NH-O complex passes through a low barrier of 2.7 kcal/mol (2.3 kcal/mol with respect to the initial reactants) at TS7 to yield the $NH_2 + OH$ products. At the MRCI/6-311+G(3df,-2p) level, the relative energy of TS7 is slightly higher, 3.4 kcal/mol, but the difference is not very significant. Therefore, H_2NH-O is likely to be a short-lived intermediate, even if it exists. RRKM calculations gave the microcanonical rate constant for the decomposition of H_2NH-O via TS7 as $\sim 1.0 \times 10^{11}$ s^{-1}. If the complex does not exist, the direct abstraction reaction mechanism on the first excited PES can be described as $O(^1D) + NH_3 \rightarrow TS7 \rightarrow NH_2 + OH$. Thus, we can conclude that the $O(^1D) + NH_3 \rightarrow H_2NH-O \rightarrow TS7 \rightarrow NH_2 + OH$ addition/abstraction or the $O(^1D) + NH_3 \rightarrow TS7 \rightarrow NH_2 + OH$ direct abstraction pathway is expected to partly contribute to the OH formation channel and, to some extent, to account for the

forward scattering of these products in the molecular beam experiment.[4] The abstraction mechanism can lead to the formation of the forward-scattered products only at collision energies higher than 2.3 kcal/mol, unless quantum mechanical tunneling occurs through the barrier at TS7.

Alternatively, the forward-scattered products can be formed on the ground-state PES through the trajectories that bypass the long-lived NH_2OH intermediate and lead to the $NH_2 + OH$ products via a short-lived NH_2OH complex. This dynamics possibility has been recently demonstrated for the $O(^1D) + CH_4 \rightarrow OH + CH_3$ reaction by quasi-classical trajectory (QCT) calculations of Sayos et al.[32] and direct ab initio dynamics simulations of Yu and Muckerman.[33] Both studies consistently show that, even if only the ground electronic state trajectories are considered, the differential cross section for the direct reaction exhibits a pronounced forward peak superimposed on a relatively isotropic background. The question about the relative importance of the three reaction mechanisms, (i) the insertion of $O(^1D)$ into an N−H bond with the formation of the long-lived NH_2OH intermediate followed by the N−O bond cleavage (ground-state PES, isotropic products); (ii) the insertion leading to a short-lived NH_2OH complex that immediately decomposes to the $OH + NH_2$ products (ground-state PES, forward-scattered products); and (iii) the direct abstraction pathway via TS7 (first excited-state PES, forward-scattered products), remains to be addressed by future dynamics simulations for the $O(^1D) + NH_3$ reaction, which should involve at least the ground and the first excited PESs. The statistical rate constants for the $NH_2OH(^1A') \rightarrow NH_2 + OH$ (6.66×10^{12} s^{-1}) and $H_2NH{-}O(^1A'') \rightarrow TS7 \rightarrow NH_2 + OH$ (1.0×10^{11} s^{-1}) channels calculated here cannot be used directly to determine branching ratios of OH produced through the insertion and addition/abstraction mechanisms. The calculated binding energy of $H_2NH{-}O$ is only 0.4 kcal/mol, and the existence of this complex could be an artifact of the theoretical method applied. If the complex does not exist, $O(^1D) + NH_3 \rightarrow TS7 \rightarrow NH_2 + OH$ is a direct bimolecular reaction on the $^1A''$ PES and RRKM theory is not applicable to compute its rate. Nevertheless, it is clear that the sum of states of TS7 is significantly less than the sum of states for the variational transition state VTS4 of the ground-state $NH_2OH \rightarrow NH_2 + OH$ channel. Therefore, the reactivity on the excited state surface would be expected to be smaller than that on the ground-state PES; a similar conclusion was also made recently for the $O(^1D) + CH_4 \rightarrow OH + CH_3$ reaction.[33,34]

4. Conclusions

The $O(^1D) + NH_3$ reaction involving vibrationally excited NH_2OH^* has been studied employing the ab initio/RRKM approach. On the basis of the calculated ground-state PES, the $O(^1D) + NH_3 \rightarrow NH_2OH \rightarrow NH_2 + OH$ channel is found to be the most favorable energetically and $NH_2 + OH$ are predicted to be the major products. The calculated relative branching ratios are 89.54% for the $NH_2 + OH$ channel, 4.25% for the H elimination, 6.10% for $NH + H_2O$, and 0.10% for $NOH + H_2$. These results are in good agreement with the experimental values, 10% for $H + NHOH/NH_2O$ and 90% for $OH + NH_2$ channels. Therefore, we can conclude that the $O(^1D) + NH_3$ reaction mainly occurs through decomposition of the long-lived complex NH_2OH^* produced by the insertion mechanism.

The $O(^1D) + NH_3$ reaction on the first singlet excited $^1A''$ PES is studied using the MRCI(14,11)/aug-cc-pVTZ//CASSCF/6-311G(d,p) level of theory. The $O(^1D) + NH_3 \rightarrow H_2NH{-}O \rightarrow TS7 \rightarrow NH_2 + OH$ channel is concluded to provide some contribution to the OH formation channel and to partially account for the forward scattering of the OH products observed in experiment.

Acknowledgment. This work was partially supported by NKBRSF, Academia Sinica, Taiwan, and Florida International University.

References and Notes

(1) Song, Y. H.; Blair, D. W.; Simiuski, V. J. *18th Symp. (Int.) Comb.*; The Combustion Institute: Pittsburgh, PA, 1981; p 53.
(2) Espinosa-Garcia, J. *J. Phys. Chem. A* **2000**, *104*, 7537.
(3) Luckhaus, D.; Scott, J. L.; Crim, F. F. *J. Chem. Phys.* **1999**, *110*, 1533.
(4) Shu, J.; Lin, J. J.; Wang, C. C.; Lee, Y. T.; Yang, X. *J. Chem. Phys.* **2001**, *115*, 842.
(5) Sumathi, R.; Sengupta, D.; Nguyen, M. T. *J. Phys. Chem. A* **1998**, *102*, 3175.
(6) Lin, M. C.; Hsu, C.-C.; Kristyan, S. *Proceedings of the 1996 JANNAF Combustion Meeting*; CPIA Publication No. 653; Laurel, MD, 1997; Vol. II, pp 419−426.
(7) Becke, A. D. *J. Chem. Phys.* **1993**, *98*, 5648.
(8) Lee, C.; Yang, W.; Parr, R. G. *Phys. Rev. B* **1988**, *37*, 785.
(9) Purvis, G. D.; Bartlett, R. J. *J. Chem. Phys.* **1982**, *76*, 1910.
(10) Bauschlicher, C. W., Jr.; Partridge, H. *J. Chem. Phys.* **1995**, *103*, 1788.
(11) Mebel, A. M.; Morokuma, K.; Lin, M. C. *J. Chem. Phys.* **1995**, *103*, 7414.
(12) Werner, H.-J.; Knowles, P. J. *J. Chem. Phys.* **1985**, *82*, 5033.
(13) Knowles, P. J.; Werner, H.-J. *Chem. Phys. Lett.* **1985**, *115*, 259.
(14) Werner, H.-J.; Knowles, P. J. *J. Chem. Phys.* **1988**, *89*, 5803.
(15) Knowles, P. J.; Werner, H.-J. *Chem. Phys. Lett.* **1988**, *145*, 514.
(16) Dunning, T. H., Jr. *J. Chem. Phys.* **1989**, *90*, 1007.
(17) MOLPRO is a package of ab initio programs written by H.-J. Werner and P. J. Knowles with contributions from J. Almlöf, R. D. Amos, M. J. O. Deegan, et al.
(18) Dalton, a molecular electronic structure program written by T. Helgaker, H. J. Aa. Jensen, J. Olsen, K. Ruud, et al.
(19) Frisch, M. J.; Trucks, G. W.; Schlegel, H. B.; Scuseria, G. E.; Robb, M. A.; Cheeseman, J. R.; Zakrzewski, V. G.; Montgomery, J. A.; Stratmann, R. E.; Burant, J. C.; Dapprich, S.; Millam, J. M.; Daniels, R. E.; Kudin, K. N.; Strain, M. C.; Farkas, O.; Tomasi, J.; Barone, V.; Cossi, M.; Cammi, R.; Mennucci, B.; Pomelli, C.; Adamo, C.; Clifford, S.; Ochterski, J.; Petersson, G. A.; Ayala, P. Y.; Cui, Q.; Morokuma, K.; Salvador, P.; Dannenberg, J. J.; Malick, D. K.; Rabuck, A. D.; Raghavachari, K.; Foresman, J. B.; Cioslowski, J.; Ortiz, J. V.; Baboul, A. G.; Stefanov, B. B.; Liu, G.; Liashenko, A.; Piskorz, P.; Komaromi, I.; Gomperts, R.; Martin, R. L.; Fox, D. J.; Keith, T.; Al-Laham, M. A.; Peng, C. Y.; Nanayakkara, A.; Challacombe, M.; Gill, P. M. W.; Johnson, B.; Chen, W.; Wong, M. W.; Andres, J. L.; Gonzalez, C.; Head-Gordon, M.; Replogle, E. S.; Pople, J. A. *Gaussian 98*, revision A.11; Gaussian, Inc.: Pittsburgh, PA, 2001.
(20) Eyring, H.; Lin, S. H.; Lin, S. M. *Basic Chemical Kinetics*; Wiley: New York, 1980.
(21) Robinson, P. J.; Holbrook, K. A. *Unimolecular Reactions*; Wiley: New York, 1972.
(22) Steinfeld, J. I.; Francisco, J. S.; Hase, W. L. *Chemical Kinetics and Dynamics*; Prentice Hall: Englewood Cliffs, NJ, 1999.
(23) Lee, H. Y.; Mebel, A. M.; Lin, S. H. *Int. J. Quantum Chem.* **2002**, *90*, 566.
(24) Lee, H. Y.; Kislov, V. V.; Lin, S. H.; Mebel, A. M.; Neumark, D. M. *Chem.-Eur. J.* **2003**, *9*, 726.
(25) Kislov, V. V.; Nguyen, T. L.; Mebel, A. M.; Lin, S. H.; Smith, S. C. *J. Chem. Phys.* **2004**, *120*, 7008.
(26) Davidson, J. A.; Schiff, H. I.; Streit, G. E.; McAfee, J. R.; Schmeltekopf, A. L. Howard, C. J. *J. Chem. Phys.* **1977**, *67*, 5021.
(27) DeMore, W. B.; Sander, S. P.; Golden, D. M.; Hampson, R. F.; Kurylo, M. J.; Howard, C. J.; Ravishankara, A. R.; Kolb, C. E.; Molina, M. J. *Chemical kinetics and photochemical data for use in stratospheric modeling. Evaluation number 12*; JPL Publication 97-4; 1997; pp 1−266.
(28) *NIST Chemistry Webbook, NIST Standard Reference DataBase Number 69*; March 2003 Release (http://webbook.nist.gov/chemistry/).
(29) Anderson, W. R. *Combust. Flame* **1999**, *117*, 394.
(30) Xia, W. S.; Zhu, R. S.; Lin, M. C.; Mebel, A. M. *Faraday Discuss.* **2001**, *119*, 191.
(31) Nguyen, T. L.; Mebel, A. M.; Lin, S. H. *J. Chem. Phys.* **2001**, *114*, 10816.
(32) Sayós, R.; Hernando, J.; Puyuelo, M. P.; Enríquez, P. A.; González, M. *Phys. Chem. Chem. Phys.* **2002**, *4*, 288.
(33) Yu, H.-G.; Muckerman, J. T. *J. Phys. Chem.* **2004**, *108*, 8615.
(34) Hernando, J.; Millán, J.; Sayós, R.; González, M. *J. Chem. Phys.* **2003**, *119*, 9504.